5530 *Inorg. Chem.* **2010**, *49*, 5530–5541
DOI: 10.1021/ic1003484

Inorganic Chemistry
Article

Study of the Coordination Abilities of Stibine Ligands to Gold(I)

Vilma R. Bojan,[†] Eduardo J. Fernández,[†] Antonio Laguna,[‡] José M. López-de-Luzuriaga,*[,†] Miguel Monge,[†] M. Elena Olmos,[†] Raquel C. Puelles,[†] and Cristian Silvestru*[,§]

[†]*Departamento de Química, Universidad de la Rioja, Grupo de Síntesis Química de La Rioja UA-CSIC Complejo Científico Tecnológico, 26004 Logroño, Spain,* [‡]*Departamento de Química Inorgánica, Instituto de Ciencia de Materiales de Aragón, Universidad de Zaragoza-CSIC, 50009 Zaragoza, Spain, and* [§]*Facultatea de Chimie si Inginerie Chimica, Universitatea Babes-Bolyai, 400028 Cluj-Napoca, Romania*

Received February 22, 2010

The reaction of [AuCl(tht)] (tht = tetrahydrothiophene) with $SbMes_nPh_{3-n}$ (n = 3 (**1**), 2 (**2**), 1 (**3**)) produces the 1:1 adducts $[AuCl(SbMes_nPh_{3-n})]$ (n = 3 (**4**), 2 (**5**), 1 (**6**)), with a Sb−Au−Cl environment, regardless of the molar ratio used (1:1 to 1:4). Addition of the same stibines to $[Au(tht)_2]ClO_4$ (molar ratio 1:1 to 1:4) results in isolation of the 1:2 adducts $[Au(SbMes_nPh_{3-n})_2]ClO_4$ (n = 3 (**7**), 2 (**10**)), containing linear Sb−Au−Sb fragments, or the 1:3 adduct $[Au(SbMesPh_2)_3]ClO_4$ (**11**), with a *quasi* trigonal planar $AuSb_3$ core. The same 1:2 cations are produced when $[Au(tht)_2]CF_3SO_3$ is reacted with **1** or following a rearrangement process when **4** is treated with $AgSbF_6$, that is, $[Au(SbMes_3)_2]X$ (X = CF_3SO_3 (**8**), SbF_6 (**9**)). The compounds were characterized by spectroscopic methods, and the molecular structures of **2**−**4**, **7**, **8**·2$CDCl_3$, **9**, and **11** were established by single-crystal X-ray diffraction. Theoretical calculations were carried out on model systems of type ER_3 and $[Au(ER_3)_n]^+$ (E = P or Sb; R = Ph or Mes; n = 2, 3, or 4) to gain insight into the bonding nature of SbR_3 ligands in homoleptic gold-stibine adducts, in comparison with phosphine-gold(I) compounds. Steric effects govern the coordination of stibines with mesityl substituents. A preference for higher coordination numbers is observed for $SbPh_3$ when compared with PPh_3 and experimentally observed C−Sb−C and Sb−C structural distortions of stibines upon coordination are reproduced theoretically.

Introduction

The use of organoantimony(III) compounds as ligands for transition metals has often been reviewed[1−9] together with analogous compounds of the other Group 15 elements. Important differences in the coordination potential of organoantimony compounds with respect to their lighter phosphorus congeners are generally related to lower stability of the Sb−C bond, weaker Lewis basicity and a greater tendency for higher coordination.[7] However, the studies reported in the last two decades on transition metal complexes have proven that stibine ligands are not simply "weakly coordinating phosphines",[8] but that they can exhibit different coordination chemistry when appropriate organic groups are attached either to antimony or to the transition metal moiety.

The ability of pnicogen ligands to form stable $M_{transition}-ER_3$ (E = P, As, Sb, Bi) complexes is controlled by electronic and steric factors.[2,3,8] The $M_{transition}-E$ bond in such complexes is basically of covalent coordination nature. For an $M-PR_3$ bond, in addition to σ donation of the lone pair of electrons from pnicogen to the metal, a π component involves transfer of metal electron density into a P−C σ^* orbital or a symmetry allowed combination of P−C σ^* and 3d orbitals.[2,8,10] As group 15 is descended the separation in the energy of *n*s and *n*p orbitals increases and, as a consequence, the E−C bonds in ER_3 have a higher p character and the lone pair has a higher s character, and is thus less available for σ coordination.[8] This model explains the following general trend in Lewis basicity: $NR_3 > PR_3 > AsR_3 > SbR_3 > BiR_3$. An increase of the C−Sb−C bond angles for the coordinated SbR_3 groups with respect to the free ligands was noted, and this behavior was rationalized in terms of a change in coordination from a predominantly Sb

*To whom correspondence should be addressed. E-mail: josemaria.lopez@unirioja.es (J.M.L.), cristi@chem.ubbcluj.ro (C.S.).

(1) McAuliffe, C. A.; Levason, W. In *Phosphine, Arsine and Stibine Complexes of the Transition Elements*; Vol. *1*, Elsevier: North-Holland, 1979.
(2) McAuliffe, C. A. In *Comprehensive Coordination Chemistry I*; Wilkinson, G., Gillard, R. D., McCleverty, J. A., Eds.; Pergamon Press: Oxford, 1987; Vol. *2*, pp 989−1066.
(3) Champness, N. R.; Levason, W. *Coord. Chem. Rev.* **1994**, *133*, 115.
(4) Breunig, H. J.; Rösler, R. *Coord. Chem. Rev.* **1997**, *163*, 33.
(5) Godfrey, S. M.; McAuliffe, C. A.; Mackie, A. G.; Pritchard, R. G. In *Chemistry of Arsenic, Antimony and Bismuth*; Norman, N. C., Ed.; Blackie Academic & Professional: London, 1998; pp 159−205.
(6) Whitmire, K. H. In *Chemistry of Arsenic, Antimony and Bismuth*; Norman, N. C., Ed.; Blackie Academic & Professional: London, 1998; pp 345−402.
(7) Breunig, H. J.; Ghesner, I. *Adv. Organomet. Chem.* **2003**, *49*, 95.
(8) Levason, W.; Reid, G. *Coord. Chem. Rev.* **2006**, *250*, 2565.
(9) Gimeno, M. C.; Laguna, A. In *Comprehensive Coordination Chemistry II*; McCleverty, J. A., Meyer, T. J., Eds.; Elsevier: New York, 2003; Vol. *6*, pp 911−1145.
(10) Orpen, A. G.; Connelly, N. G. *Organometallics* **1990**, *9*, 1206.

Published on Web 05/19/2010

p^3 hybridization in the SbC_3 group toward an sp^3 model.[8] In addition, the decrease in electronegativity of the pnicogen and more diffuse orbitals are usually considered to reduce π-back bonding for the heavier SbR_3 analogues.[8] Although reasonable, it is worth mentioning that, as far as we are aware, no theoretical treatment of the bonding abilities of stibine ligands toward transition metals that confirm these proposals has been reported to date.

On the other hand, the steric effects of pnicogen ligands are usually treated using Tolman's cone angle model which was introduced to discuss the properties of phosphine ligands,[11] but extended later to cover heavier pnicogen ligands.[2] It was shown that the cone angles of the SbR_3 derivatives are generally a few degrees smaller than those of the related PR_3 analogues,[2] and this behavior was often used to explain the higher coordination number in stibine complexes of transition metals.

Gold(I) chemistry has been governed by the concept that gold is a typical soft Lewis acid which forms its most stable compounds with relatively soft Lewis bases. While a great number of gold(I)-phosphine adducts are known, examples of gold(I)-arsine complexes are much less documented and are limited to a few examples of mononuclear and dinuclear derivatives.[6,12−16] Moreover, the chemistry of gold(I) with stibine ligands has been far less explored, and very few compounds containing gold−antimony bonds were structurally characterized.[17] Thus, although the first gold(I) complex, $[AuCl(SbEt_3)]$, was reported more than 150 years ago,[18] gold(I)-stibine chemistry has been developing very slowly.[9] Most compounds reported so far are mononuclear 1:1 adducts of the type $[Au(SbR_3)X]$ (X = halide, NCS, or organic group).[9] Dinuclear species such as $[(AuCl)_2\{\mu\text{-}(Ph_2Sb)_2CH_2\}]$[19] or $[(AuCl)_2\{\mu\text{-}1,2\text{-}(Me_2SbCH_2)_2C_6H_4\}]$[20] were also described. Examples of 1:2 adducts are, for example, $[AuCl\{Sb(C_6H_4Me\text{-}3)_3\}_2]$[21] and $[AuCl(SbPh_3)_2]$.[22] The reaction of [AuR(tht)] with $SbPh_3$ also resulted in compounds of stoichiometry 1:2, and an equilibrium between the neutral three-coordinate $[AuR(SbPh_3)_2]$ and the ionic $[Au(SbPh_3)_4][AuR_2]$ species has been proposed in solution ($R = C_6F_5$,[23−25] C_6Cl_5,[26] 4,4′-$HC_6F_4-C_6F_4$,[27] 2-$(O_2N)C_6H_4$,[28] 2,4,6-$(O_2N)_3C_6H_2$,[29]). The related $[Au(SbPh_3)_4]ClO_4$ was easily obtained by treating $[Au(tht)_2]ClO_4$ with $SbPh_3$.[30] More recently the ionic complexes $[Au(dmsm)_2]PF_6$ and $[Au(dpsm)_2]PF_6$ (dmsm = $Me_2SbCH_2SbMe_2$, dpsm = $Ph_2SbCH_2SbPh_2$) were synthesized by reacting [AuCl(tht)], distibine ligands, and $TlPF_6$, in a 1:2:1 molar ratio, in CH_2Cl_2.[31] Unfortunately, in most cases the low stability of the compounds prevents complete characterization, and until a few years ago only three ionic compounds containing the same complex cation, that is, $[Au(SbPh_3)_4]X$ (X = $[Au(C_6F_5)_2]^-$,[24] $[Au\{C_6H_2(NO_2)_3\text{-}2,4,6\}_2]^-$,[29] ClO_4^{-}[32]), had had their molecular structure determined by single-crystal X-ray diffraction. In the solid state, regardless of the nature of the counteranion, the $[Au(SbPh_3)_4]^+$ cations show an almost tetrahedral coordination at the gold center, with Sb−Au−Sb bond angles ranging between 107.8 to 111.0° and Au−Sb bond lengths between 2.585(1) and 2.669(1) Å.

The structures of two new gold−antimony compounds were recently described. We have reported on the ionic complex $[Au_2\{(Ph_2Sb)_2O\}_3](ClO_4)_2$, whose cation shows two gold centers in a trigonal-planar environment as a result of the bridging nature of the Sb donor ligands. The Au−Sb bond distances were slightly shorter than those found in the tetracoordinate $[Au(SbPh_3)_4]^+$ cations, as expected for a lower coordination number.[33] The other compound is a polynuclear complex, $[Au_8(Et_3P)_6(SbPh)_2(SbPh_2)_4]$, which consists of a distorted heterocubic central $[Au_6Sb_2]$ unit connected on two opposite edges by two Sb−Au−Sb fragments. All gold atoms exhibit tetrahedral coordination, but as part of different cores, that is, AuP_2Sb_2, $AuPSb(Au)_2$ and $AuSb_2(Au)_2$.[34]

Using the possibility to modulate the steric and electronic properties of SbR_3 ligands by changing the nature of the organic groups on antimony, we decided to investigate the possibility to obtain gold-stibine adducts of different stoichiometry with the objective of carrying out theoretical calculations of the type ONIOM DFT/UFF. With these we expect to gain insight into the bonding abilities of stibine ligands containing different aryl substituents (phenyl or mesityl) toward gold(I). We will also try to explain the observed experimental differences between phosphine and stibine on coordination to the gold(I) center, paying special attention to the coordination environment. Finally, the calculations will also be focused on an explanation of the previously mentioned structural distortions, with reference to the E−C distances and C−E−C angles (E = Sb or P) when the ligands bind the metal centers.

(11) (a) Tolman, C. A. *J. Am. Chem. Soc.* **1970**, *92*, 2956. (b) Tolman, C. A. *Chem. Rev.* **1977**, *77*, 313.
(12) Akrivos, D.; Katsikis, H. J.; Koumoutsi, A. *Coord. Chem. Rev.* **1997**, *167*, 95.
(13) Gimeno, M. C.; Laguna, A. *Chem. Rev.* **1997**, *97*, 511.
(14) Laguna, A. In *Gold − Progress in Chemistry, Biochemistry and Technology*; Schmidbaur, H., Ed.; Wiley: New York, 1999; pp 349−427.
(15) Schmidbaur, H.; Grohmann, A.; Olmos, M. E.; Schier, A. In *The Chemistry of Organic Derivatives of Gold and Silver*; Patai, S., Rappoport, Z., Eds.; Wiley: Chichester, 1999; pp 227−311.
(16) Fernández, E. J.; Laguna, A.; Olmos, M. E. *Adv. Organomet. Chem.* **2005**, *52*, 77.
(17) Silvestru, C. Gold-Metal Interactions and Aplications. In *Modern Supramolecular Gold Chemistry*; Laguna, A., Ed.; Wiley-VCH: Weinheim, 2008; pp 181−293.
(18) von Hofmann, A. W. *Justus Liebigs Ann. Chem.* **1857**, *103*, 357.
(19) Chiffey, A. F.; Evans, J.; Lavason, W.; Webster, M. *Polyhedron* **1996**, *15*, 591.
(20) Levason, W.; Matthews, M. L.; Reid, G.; Webster, M. *Dalton Trans.* **2004**, 554.
(21) McAuliffe, C. A.; Parish, R. V. D.; Randall, P. D. *J. Chem. Soc., Dalton Trans.* **1979**, 1730.
(22) Bovio, B.; Bonati, F.; Burini, A.; Pietroni, B. R. *Z. Naturforsch.* **1984**, *39b*, 1747.
(23) Usón, R.; Laguna, A.; Vicente, J.; García, J.; Jones, P. G.; Sheldrick, G. M. *J. Chem. Soc., Dalton Trans.* **1981**, 655.
(24) Jones, P. G. *Z. Naturforsch.* **1982**, *37b*, 937.
(25) Moss, K.; Parish, R. V. D.; Laguna, A.; Laguna, M.; Usón, R. *J. Chem. Soc., Dalton Trans.* **1983**, 2071.
(26) Usón, R.; Laguna, A.; de la Orden, M. U.; Arrese, M. L. *Synth. React. Inorg. Met.-Org. Chem.* **1984**, *14*, 369.
(27) Usón, R.; Laguna, A.; Laguna, M.; Colera, I.; De Jesús, E. *J. Organomet. Chem.* **1984**, *263*, 121.
(28) Vicente, J.; Arcas, A.; Mora, M.; Solans, X.; Font-Altaba, M. *J. Organomet. Chem.* **1986**, *309*, 369.
(29) Vicente, J.; Arcas, A.; Jones, P. G.; Lautner, J. *J. Chem. Soc., Dalton Trans.* **1990**, 451.
(30) Usón, R.; Laguna, A.; Navarro, A.; Parish, R. V.; Moore, L. S. *Inorg. Chim. Acta* **1986**, *112*, 205.
(31) Even, T.; Genge, A. R. J.; Hill, A. M.; Holmes, N. J.; Levason, W.; Webster, M. *J. Chem. Soc., Dalton Trans.* **2000**, 655.
(32) Jones, P. G. *Acta Crystallogr.* **1992**, *C48*, 1487.
(33) Bojan, V. R.; Fernández, E. J.; Laguna, A.; López-de-Luzuriaga, J. M.; Monge, M.; Olmos, M. E.; Silvestru, C. *J. Am. Chem. Soc.* **2005**, *127*, 11564.
(34) Fenske, D.; Rothenberger, A.; Wieber, S. *Eur. J. Inorg. Chem.* **2007**, 3469.

Table 1. Selected Bond Lengths [Å] and Angles [deg] for Compounds **2** and **3**

2		**3**	
Sb(1)−C(1)	2.178(6)	Sb(1)−C(1)	2.155(7)
Sb(1)−C(10)	2.177(6)	Sb(1)−C(10)	2.153(8)
Sb(1)−C(19)	2.147(6)	Sb(1)−C(16)	2.165(6)
C(1)−Sb(1)−C(10)	102.3(2)	C(1)−Sb(1)−C(10)	100.9(3)
C(1)−Sb(1)−C(19)	106.8(2)	C(1)−Sb(1)−C(16)	97.8(2)
C(10)−Sb(1)−C(19)	97.0(2)	C(10)−Sb(1)−C(16)	98.7(3)

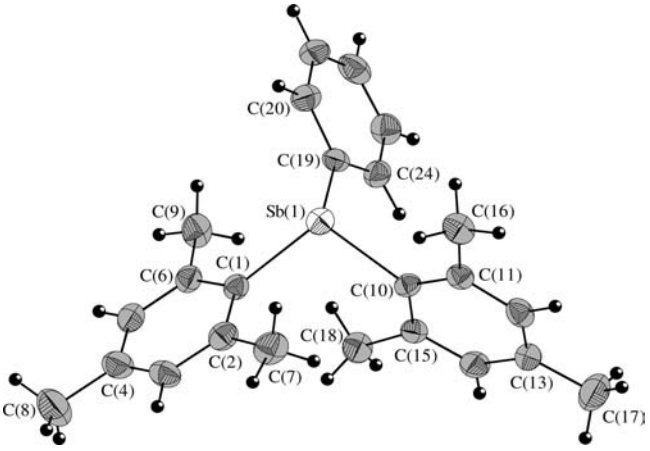

Figure 1. ORTEP representation at 30% probability and atom numbering scheme for compound **2**.

Results and Discussion

A first strategy arises from the idea that the increase in bulk of a substituent group on antimony in SbR_3 will increase the C−Sb−C angle, which will increase the p character of the lone pair. Thus, more electron density will be available at the antimony atom and less stibine units will be required to satisfy the electron deficiency of the gold(I) atom. In this sense, the *mesityl* group is a good candidate for such studies and, in addition, the electron donating methyl groups in this aromatic substituent are expected to increase the donor properties of the stibine ligand toward the metal center in comparison with the predominantly used $SbPh_3$ analogue. On the other hand, to diminish the strain of sterically demanding ligands, it would be very useful if the gold atom remained coordinatively unsaturated, thus resulting in adducts with different stoichiometry.

The new stibines $SbMes_2Ph$ (**2**) and $SbMesPh_2$ (**3**) were prepared, and their molecular structures were established by single-crystal X-ray diffraction from single crystals obtained by slow evaporation of an hexane solution of the materials. A selection of bond lengths and angles is given in Table 1. As for the homoleptic $SbMes_3$ (**1**)[35] and $SbPh_3$[36] derivatives, the coordination geometry of the antimony atom in the heteroleptic stibines **2** and **3** is trigonal pyramidal (Figures 1 and 2).

A comparison of the structural parameters revealed the expected increase of averaged C−Sb−C angle with each additional substitution of a phenyl group by a mesityl group, that is, $SbPh_3$ (96.0°) < $SbMesPh_2$ (**3**) (99.1°) < $SbMes_2Ph$ (**2**) (102.0°) < $SbMes_3$ (**1**) (105.6°). This behavior suggests that as the number of mesityl groups on antimony increases, less stibine ligands are expected to coordinate to a gold atom, for steric reasons. This effect would parallel the effect because of a potential increase in electron density available for donation from the antimony atom.

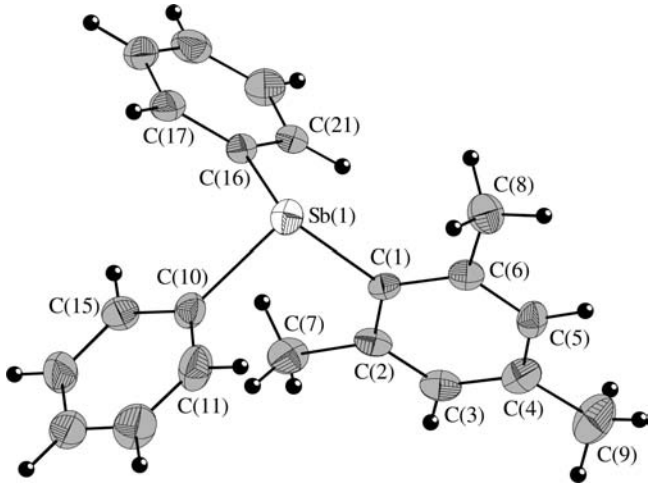

Figure 2. ORTEP representation at 30% probability and atom numbering scheme for compound **3**.

Scheme 1. Reaction Scheme for the Synthesis of Gold(I) Complexes **4**−**11**

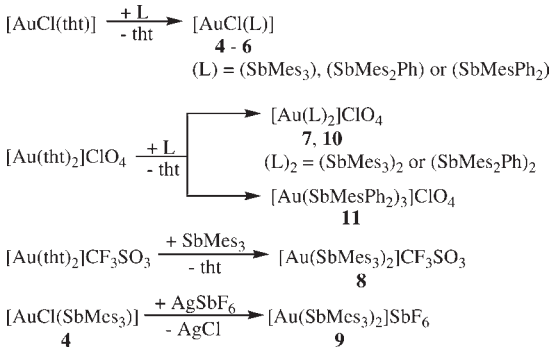

The reaction of [AuCl(tht)] with stibines **1**−**3** resulted in the isolation of the 1:1 adducts [AuCl(L)] (L = $SbMes_3$ (**4**), $SbMes_2Ph$ (**5**), $SbMesPh_2$ (**6**)) (Scheme 1), as white solids, soluble in CH_2Cl_2, $CHCl_3$, acetone, and tetrahydrofuran. Although it was expected that less bulky stibines, for example, $SbMesPh_2$, would favor an increase in the gold(I) atom's coordination number, only the 1:1 adducts could be isolated regardless of the molar ratio of the starting materials (1:1 to 1:4). For all three compounds the ES+ mass spectra show the $[Au(L)_2]^+$ fragment as base peak, because of a recombination process during fragmentation of the 1:1 adducts **4**−**6**.

Therefore, to achieve the coordination of further stibine moieties to the gold(I) center, another strategy was used, that is, the reaction of the ionic $[Au(tht)_2]ClO_4$ derivative with stibines **1**−**3**. Using the bulkier $SbMes_3$ (**1**) and $SbMes_2Ph$ (**2**), the ionic $[Au(L)_2]ClO_4$ (L = $SbMes_3$ (**7**), $SbMes_2Ph$ (**10**)) species were isolated (Scheme 1). Regardless of the molar ratio used in the reaction between the $[Au(tht)_2]ClO_4$ and **1**, complex **7** was always isolated, suggesting the bulkiness of the stibine controls the number of stibine units coordinated to the gold(I) center. By contrast, the less sterically demanding stibine **3** produced the ionic $[Au(SbMesPh_2)_3]ClO_4$ (**11**) species. Similarly, the reaction of $[Au(tht)_2]CF_3SO_3$ with **1** led to the formation of $[Au(SbMes_3)_2]CF_3SO_3$ (**8**), suggesting

(35) Ates, M.; Breunig, H. J.; Ebert, K. H.; Kaller, R.; Drager, M.; Behrens, U. *Z. Naturforsch.* **1992**, *47b*, 503.

(36) Adams, E. A.; Kolis, J. W.; Pennington, W. T. *Acta Crystallogr.* **1990**, *C46*, 917.

Table 2. Selected Bond Lengths [Å] and Angles [deg] for Compound **4**

Au−Cl	2.2888(8)	Au−Sb	2.5100(2)
Sb−C(1)	2.142(3)	Sb−C(11)	2.141(3)
Sb−C(21)	2.144(3)	Cl−Au−Sb	177.39(3)
C(1)−Sb−C(11)	107.40(11)	C(1)−Sb−C(21)	109.41(11)
C(11)−Sb−C(21)	113.80(12)	Au−Sb−C(1)	113.06(8)
Au−Sb−C(11)	105.32(8)	Au−Sb−C(21)	107.90(8)

Table 3. Selected Bond Lengths [Å] and Angles [deg] for Compounds **7**, **8**·2CDCl$_3$, and **9**

	7	**8**·2CDCl$_3$	**9**
Au−Sb(1)	2.5855(3)	2.5591(4)	2.5806(18)
Au−Sb(2)		2.5629(4)	
Sb(1)−C(1)	2.142(5)	2.151(5)	2.151(16)
Sb(1)−C(11) [a]	2.146(6)	2.146(5)	2.135(12)
Sb(1)−C(21) [a]	2.136(6)	2.140(5)	2.114(14)
Sb(2)−C(31)		2.155(5)	
Sb(2)−C(41)		2.142(5)	
Sb(2)−C(51)		2.147(5)	
Sb(1)−Au−Sb(2) [a]	173.10(2)	174.801(15)	178.10(6)
C(1)−Sb(1)−C(11) [a]	115.02(19)	112.84(19)	113.6(5)
C(1)−Sb(1)−C(21) [a]	111.53(18)	110.04(19)	109.0(6)
C(11)−Sb(1)−C(21) [a]	103.82(19)	111.46(19)	105.6(5)
C(31)−Sb(2)−C(41)		109.30(19)	
C(31)−Sb(2)−C(51)		113.33(19)	
C(41)−Sb(2)−C(51)		107.35(19)	
Au−Sb(1)−C(1) [a]	110.15(14)	107.57(13)	109.6(4)
Au−Sb(1)−C(11) [a]	104.98(13)	103.99(13)	107.2(3)
Au−Sb(1)−C(21) [a]	111.02(14)	110.72(13)	111.9(4)
Au−Sb(2)−C(31)		110.20(13)	
Au−Sb(2)−C(41)		109.00(14)	
Au−Sb(2)−C(51)		107.54(13)	

[a] C(11), C(21), and Sb(2) are C(10), C(21), and Sb(1a) for **9**.

that the formation of the $[Au(SbMes_3)_2]^+$ cation is not dependent on the counteranion. Moreover, when **4** was reacted with $AgSbF_6$, the $[Au(SbMes_3)_2]SbF_6$ (**9**) species was isolated as result of a redistribution process, thus providing further evidence for the high stability of the $[Au(SbMes_3)_2]^+$ cation. All these ionic species were isolated as white solids, soluble in CH_2Cl_2, $CHCl_3$, acetone, and tetrahydrofuran. Usually the gold(I) compounds described in this work decompose when left for up to 1 day at room temperature.

The compounds were characterized by NMR spectroscopy in solution, as well as IR spectroscopy and mass spectrometry. The IR spectra for compounds **4**−**6** are consistent with the presence of a covalent Au−Cl bond, while those for the ionic compounds **7**, **10**, and **11** indicate the presence of the perchlorate ion. In most cases the bands corresponding to the Au−Cl bond and ClO_4^- anion, respectively, suffer slight shifts compared with the gold(I) starting materials.

Mass spectra were expected to provide evidence for the nature of the isolated complexes. However, no fragment corresponding to the molecular ion was obtained in the ES+/MS spectra of the 1:1 adducts **4**−**6**, and the base peak was always found to be the cation $[Au(L)_2]^+$. This behavior, which might be explained by fragmentation of the parent compound and recombination of the $[Au(L)]^+$ cation with a further stibine fragment, suggests that ionic compounds might be stable enough to attempt their preparation, and this was later confirmed by the isolation of the ionic derivatives described in this work. For compound **11** no evidence of a fragment containing three antimony atoms and one gold was found in the ES+/MS spectrum, and again the fragment of highest mass was $[Au(SbMesPh_2)_2]^+$.

Table 4. Selected Bond Lengths [Å] and Angles [deg] for Compound **11**[a]

Au−Sb	2.6250(4)	Sb−C(11)	2.125(7)
Sb−C(1)	2.145(7)	Sb−C(21)	2.134(7)
Sb−Au−Sb(a)	119.524(3)		
C(1)−Sb−C(11)	100.4(2)	Au−Sb−C(1)	119.42(17)
C(1)−Sb−C(21)	110.6(2)	Au−Sb−C(11)	119.54(16)
C(11)−Sb−C(21)	98.7(2)	Au−Sb−C(21)	106.19(16)

[a] Symmetry transformations used to generate equivalent atoms: "a" *z*, *x*, *y*.

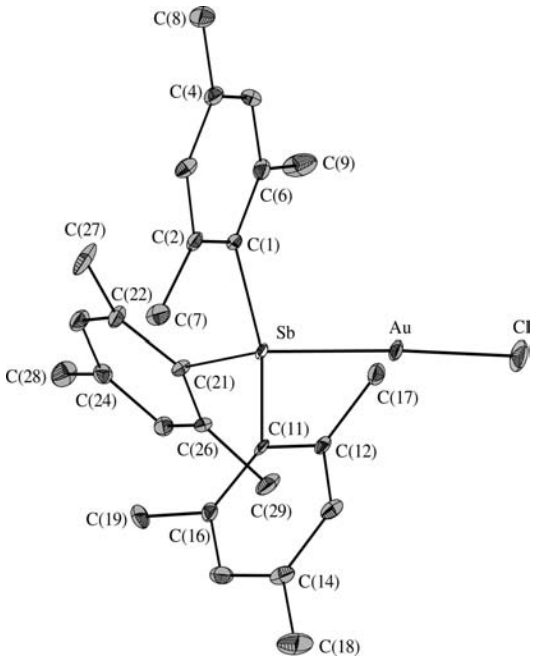

Figure 3. ORTEP representation at 50% probability and atom numbering scheme for complex **4**. H atoms are omitted for clarity.

The investigation of the title gold(I) compounds in solution by means of NMR spectroscopy was difficult because of very fast decomposition, even when freshly prepared compounds were used. In many cases gold mirrors were formed during the measurements. The presence of the triorganostibine moieties as ligands were confirmed from the NMR spectra in each case. It should also be noted that the chemical shifts for the ligands in the gold complexes were shifted with respect to the free stibines, a behavior considered indicative of the coordination of antimony to the gold center. Regardless of the nature of compounds, only one set of ^1H and ^{13}C resonances is observed for same organic groups in a molecular unit, for example, six carbon resonances for $[AuCl(SbMes_3)]$ (**4**) or $[Au(SbMes_3)_2]ClO_4$ (**7**), suggesting not only equivalence of mesityl groups in a stibine ligand (as in **4**), but also equivalence of the stibine moieties coordinated to a gold atom (as in **7**). The presence of the fluorinated anions in **8** and **9** was confirmed by a singlet resonance in the ^{19}F NMR spectra.

Crystals of the gold(I) compounds, suitable for the determination of the molecular structure by single-crystal X-ray diffraction, were obtained from CH_2Cl_2/hexane (for **4**, **7**, **9**, and **11**) or $CDCl_3$ (for **8**·2CDCl$_3$), at −20 °C. A selection of bond lengths and angles for these compounds is given in Tables 2−4.

The crystal structure of compound **4** contains monomeric units in which one stibine ligand is bonded to the AuCl unit

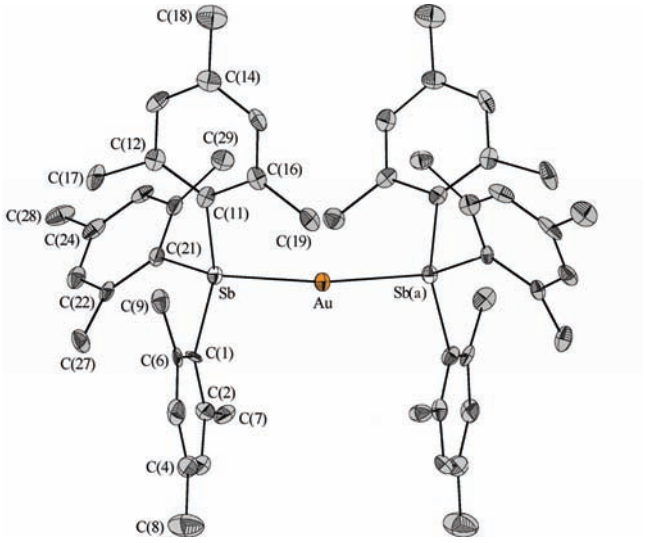

Figure 4. ORTEP representation at 50% probability and atom numbering scheme for the cation of complex **7**. Sb(a) (x, y, $-z$). H atoms are omitted for clarity.

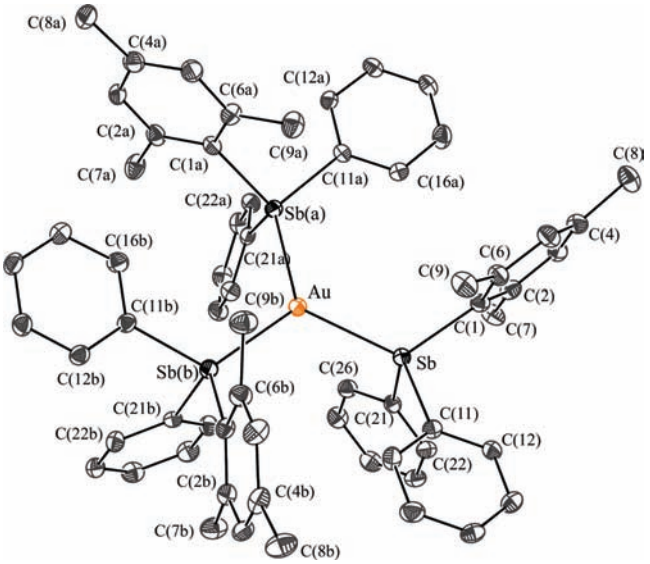

Figure 5. Structure of the cation of complex **11**. Sb(a) (z, x, y); Sb(b) (y, z, x). H atoms are omitted for clarity.

(Figure 3). The gold center is two-coordinated with almost linear geometry (Cl−Au−Sb 177.39(3)°). The Au−Cl bond length of 2.2888(8) Å is of the same magnitude as those observed in the isomorphous [AuCl(PMes$_3$)] derivative (Au−Cl 2.271(22) Å).[37] The Au−Sb bond length (2.5100(2) Å) is considerably shorter than those in the trigonal $AuSb_3$ system of $[Au_2\{(Ph_2Sb)_2O\}_3](ClO_4)_2$ (2.6048(5)−2.6173(5) Å)[33] or the tetrahedral cation of $[Au(SbPh_3)_4]ClO_4$ (2.658(2)−2.656(2) Å),[32] as expected for a lower coordination number.

The molecular structure of **6** was also determined from crystals grown from $CHCl_3$/hexane, showing very similar parameters as in **4**, although the quality of the crystals did not allow us to obtain publishable results.

The Tolman cone angle was used as a parameter for comparative studies on the steric effects of phosphorus ligands and then extended to the heavier pnicogen ligands.[2,8,11] A method described by Mingos and Müller[38] for the determination of Tolman cone angles of phosphines from crystallographic parameters, and also used for metal carbonyl complexes of Sb^{t}Bu$_3$ and Bi^{t}Bu$_3$ ligands,[39] was applied to stibines **1** and **3**. For **1** the crystallographic cone angle θ (168.3°) was found to be considerably smaller than the reported value of 205°, which was obtained without consideration of the experimentally determined M−Sb bond length.[2] As expected, the crystallographic cone angle θ is considerably larger for stibine **1** than for stibine **3** (150.2°).

Mesityl groups are expected to increase the Lewis basicity of stibines **1**−**3** but, on the other hand, trigonal 1:2 and tetrahedral 1:3 adducts are only known with the better donor ligand, PPh_3, that is, $[AuCl(PPh_3)_2]$[40] and $[AuCl(PPh_3)_3]$.[41] Only crystals of the 1:1 adducts could be isolated for stibines **1**−**3** and this behavior might be due to several reasons: (i) the general tendency for linear coordination in neutral gold(I) complexes; (ii) the ligands provide enough electron density to the neutral gold(I) center to stabilize complexes **4**−**6**; (iii) the bulkiness of the antimony ligands prevents the coordination of further stibine to the gold center. It seems that all these factors play an interactive role resulting in particular stoichiometries for particular ligands.

The ionic compounds **7**−**9** contain the cation $[Au(SbMes_3)_2]^+$ (Figure 4) in which the gold center is two-coordinated with a slightly distorted linear geometry (Sb−Au−Sb 173.10(2), 174.801(15), and 178.10(6)° for **7**, **8**·2CDCl$_3$, and **9**, respectively). The Au−Sb bond lengths (2.5855(3), 2.5591(4)/2.5629(4), and 2.5806(18) Å for **7**, **8**·2CDCl$_3$, and **9**, respectively) are intermediate between those found in the neutral 1:1 complexes **4** (2.5100(2) Å) or **6**·CHCl$_3$ (2.4999(11) Å) and in the tricoordinated $[Au_2\{(Ph_2Sb)_2O\}_3](ClO_4)_2$ (2.6048(5)−2.6173(5) Å).[33] The molecular parameters of the cation are not affected by a change in the counteranion, that is, ClO_4^- in **7**, $CF_3SO_3^-$ in **8**·2CDCl$_3$, or $[SbF_6]^-$ in **9**.

The bulkiness of stibines **1** and **2** prevents further coordination of a ligand unit to the gold(I) center. In contrast, use of the less bulky stibine **3** results in the isolation of the ionic compound **11** whose crystal structure contains the cation $[Au(SbMesPh_2)_3]^+$ with three organoantimony ligands coordinated to the gold(I) center in an almost planar trigonal arrangement (the Au atom is displaced 0.182 Å from the Sb_3 plane) (Figure 5). Surprisingly, complex **11** does not show luminescence either in solid state or in solution at room temperature or at 77 K. The slightly distorted trigonal geometry might be responsible for the absence of luminescence at room temperature although this is commonly present in tricoordinated gold(I) species. The stronger donor characteristics of the mesityl group may stabilize the LUMO, reducing the HOMO−LUMO gap and promoting the quenching of the luminescence. Another possibility for the absence of luminescence could be that the T-shaped distortion of the lowest triplet excited state responsible for the emission is not achieved because of steric hindrance.[33]

In the crystal structure of **11** the gold atom lies in a 3-fold axis, so only one stibine ligand appears in the asymmetric

(37) Bott, R. C.; Bowmaker, G. A.; Buckley, R. W.; Healy, P. C.; Senake Perera, M. C. *Aust. J. Chem.* **2000**, *53*, 175.
(38) Müller, T. E.; Mingos, D. M. P. *Transition Met. Chem.* **1995**, *20*, 533.
(39) Breunig, H. J.; Lork, E.; Raţ, C. I.; Wagner, R. P. *J. Organomet. Chem.* **2007**, *692*, 3430.
(40) (a) Baenziger, N. C.; Dittemore, K. M.; Doyle, J. R. *Inorg. Chem.* **1974**, *13*, 805. (b) Khan, M.; Oldham, C.; Tuck, D. G. *Can. J. Chem.* **1981**, *59*, 2714.
(41) Jones, P. G.; Sheldrick, G. M.; Muir, J. A.; Muir, M. M.; Pulgar, L. B. *J. Chem. Soc., Dalton Trans.* **1982**, 2123.

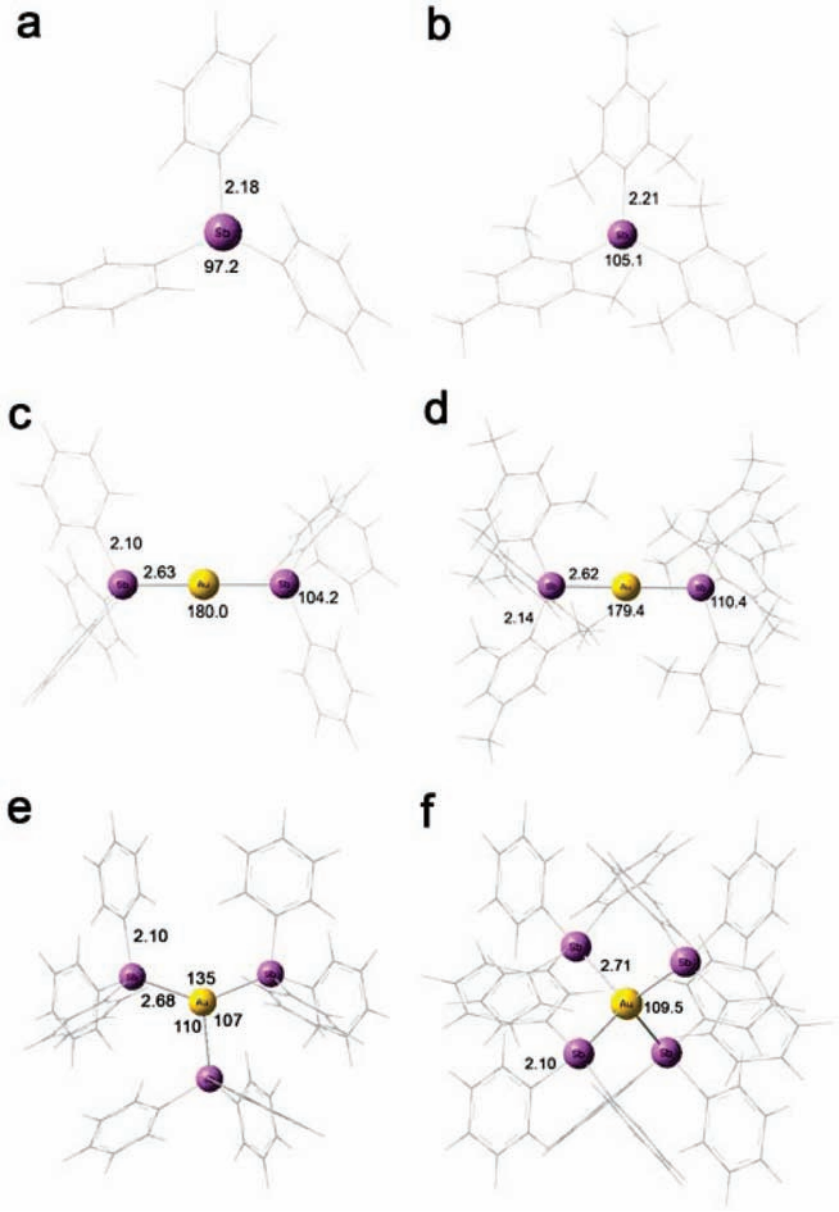

Figure 6. Fully optimized model systems with triphenylstibine (a, c, e, f) and trimesitylstibine (b, d) ligands. Similar models have been optimized for triphenylphosphine ligands.

unit. The Au−Sb bond distances in **11** (2.6250(4) Å) are longer than in the trigonal $AuSb_3$ system of $[Au_2\{(Ph_2Sb)_2O\}_3](ClO_4)_2$ (2.6048(5)−2.6173(5) Å),[33] probably because of the bulkier stibine ligand, but shorter than in the cationic $[Au(SbPh_3)_4]ClO_4$ (2.658(2)−2.656(2) Å).[32]

None of the gold(I)-stibine complexes described in this work exhibit Au(I)···Au(I) contacts or interactions between other heavy atoms. A closer check of the crystal packing revealed that, except for **11**, the gold(I) complexes established more or less complex networks through weak halogen- and/or oxygen−hydrogen contacts (cf. Σr_{vdW}(Cl,H) 3.01 Å, Σr_{vdW}(F,H) 2.55 Å; Σr_{vdW}(O,H) 2.60 Å)[42] (see Supporting Information). Thus, the molecules of **4** are associated into a waved layer through Cl···H contacts. In contrast, a 3D architecture is present in the crystal structure of **7**, with each cation being connected through O···H contacts to four different anions and vice versa. In the crystal structure of **8**·2$CDCl_3$, dimeric units are formed through Cl···H contacts between cations and solvent molecules, which are further connected into double layers by O···H contacts with anions. An interesting supramolecular architecture was found in the crystal structure of **9**, which contains the same cation as in compounds **7** and **8**·2$CDCl_3$. Here a helicoidal chain polymer with alternating cations and anions is formed through fluorine−hydrogen contacts, with no further interchain contacts established.

In the crystal structure of compound **11** there are no interactions which would influence crystal packing, the closest distance between the cations' gold centers being 11.776(3) Å.

Theoretical Calculations

As has been mentioned, the bonding characteristics of stibine ligands toward gold(I) are very interesting from a theoretical viewpoint. A theoretical confirmation together

(42) Emsley, J. In *Die Elemente*; Walter de Gruyter: Berlin, 1994.

with a plausible bonding explanation becomes an interesting challenge. Therefore, taking all the experimental structural information into account we have carried out ONIOM[43] DFT/UFF[44] calculations as implemented in Gaussian03[45] to gain insight into the bonding nature of SbR_3 ligands in homoleptic gold-stibine adducts. These were also compared with phosphine-gold(I) compounds. We have carried out theoretical calculations on model systems of the type ER_3 and $[Au(ER_3)_n]^+$ (E = P or Sb; R = Ph or Mes; n = 2, 3, or 4) (Figure 6). By making use of the ONIOM approach we have fully optimized all molecular model systems at the DFT/UFF level of theory which accounts for complete molecules, including all the ligand atoms. After optimization, all model systems were recalculated at the DFT/B3LYP level of theory to have a single point electronic structure at the optimized geometry. A summary of the already experimentally reported X-ray diffraction results, structural parameters, and the theoretical results obtained are given in Tables 5 and 6, respectively. From these results we can infer several interesting conclusions.

We first analyzed the influence of the stibine aryl groups (phenyl vs mesityl) on the coordination with Au(I) centers by NBO[53] analysis and BSSE-corrected (using the counterpoise correction)[54] Au−Sb dissociation energy calculations of two-, three-, and four-coordinated $[Au(SbR_3)_n]^+$ (R = Ph or Mes; n = 2, 3, and 4) cationic units. If we focus on the bonding abilities of $SbPh_3$ and $SbMes_3$ ligands toward gold we observe several interesting results that are comparable to the obtained experimental results. First, the fully optimized free ligands show similar structural parameters to those observed in the X-ray diffraction studies of $SbPh_3$ and $SbMes_3$, respectively. It is worth mentioning that the calculated C−Sb−C angles are very close to the experimental values, with the expected larger angle for the mesityl ligand (105.1° theoretical; 105.0° experimental) than for the phenyl ligand (97.2° theoretical; 96.0° experimental).

Table 5. Selected Experimental X-ray Diffraction Structural Parameters for Free Ligands and for Homoleptic Stibine- and Phosphine-Gold(I) Complexes $[Au(ER_3)_n]^+$ (E = P or Sb; R = Ph or Mes; n = 2, 3, or 4)

	Au−E	E−C	C−E−C	ref
$SbPh_3$		2.14−2.15	95.6−98.0	36
$SbPh_2Mes$		2.15−2.16	97.8−100.9	this work
$SbPhMes_2$		2.15−2.18	97.0−106.8	this work
$SbMes_3$		2.18−2.18	103.6−105.9	35
PPh_3		1.83−1.83	101.9−102.5	46
$PMes_3$		1.83−1.84	103.6−105.9	47
$[Au(SbPh_3)_4]^+$	2.65−2.66	2.10−2.14	99.1−102.1	32
$[Au(SbPh_2Mes)_3]^+$	2.62	2.12−2.14	98.7−110.6	this work
$[Au(SbMes_3)_2]^+$	2.58	2.14−2.15	103.8−115.0	this work
$[Au(PPh_3)_4]^+$	2.35−2.53	1.69−1.76	88.3−114.6	48, 49
$[Au(PPh_3)_3]^+$	2.37−2.40	1.80−1.83	102.9−106.5	50
$[Au(PPh_3)_2]^+$	2.31−2.31	1.78−1.81	104.6−107.5	51
$[Au(PMes_3)_2]^+$	2.35	1.82−1.83	111.5−113.3	52

Second, we analyzed the different coordination abilities of $SbPh_3$ and $SbMes_3$ toward gold in homoleptic complexes by using theoretical models of the type $[Au(SbR_3)_n]^+$ (R = Ph or Mes; n = 2, 3, and 4) (Figure 6). In the case of the $SbPh_3$ ligand, the three possible coordination environments, linear, trigonal planar, and tetrahedral, each reach a local minimum with Au−Sb dissociation energies of 53.1, 31.81, and 14.16 $kcal \cdot mol^{-1}$, respectively, and with Au−Sb distances within the range of coordination bonds (see Tables 5 and 6). In contrast, when the aryl substituent of the stibine ligand is mesityl, only the homoleptic model with two stibine ligands in a linear coordination geometry, $[Au(SbMes_3)_2]^+$, converges to a local minimum showing an Au−Sb dissociation energy of 48.3 $kcal \cdot mol^{-1}$, close to that observed with triphenylstibine. When three or four $SbMes_3$ ligands are placed around gold in the model system, the optimization run does not converge and tends to dissociate one or two stibine ligands, respectively, leading to $[Au(SbMes_3)_2]^+$ fragments. These results agree with the previously reported experimental data on $SbPh_3$ ligands and with those reported in this work for bulkier $SbMesPh_2$, $SbMes_2Ph$, and $SbMes_3$ ligands. Thus, while in the case of $SbPh_3$ it is possible to achieve tetrahedral coordination, the coordination number is reduced when mesityl substituents are included in the stibine. In the case of the complex $[Au(SbMesPh_2)_3]ClO_4$ (**11**), three stibine ligands in a trigonal planar coordination environment are observed, whereas for complexes $[Au(SbMes_2Ph)_2]ClO_4$ (**10**) or $[Au(SbMes_3)_2]ClO_4$ (**7**) two stibines in a linear coordination around the gold atom are found. If the electronic properties for the model systems $[Au(SbR_3)_2]^+$ (R = Ph or Mes) are compared, both the NBO charges on gold and antimony, and the natural electron configurations (see Table 6 and Supporting Information) are quite similar for each molecule. Therefore, it seems that the coordination environment is governed by steric effects rather than electronic ones.

Another interesting feature is the different bonding of PPh_3 and $SbPh_3$ ligands to Au(I) in homoleptic complexes. We have analyzed this theoretically by using model systems of the type $[Au(EPh_3)_n]^+$ (E = P or Sb; n = 2, 3, and 4). With these calculations we try to reproduce the observed experimental tendency in which the number of PPh_3 ligands bonded to gold is usually 2 (linear) or 3 (trigonal planar) and, to a lesser extent, 4, whereas in the case of $SbPh_3$ only one type of coordination environment consisting of 4 $SbPh_3$ ligands in a

(43) Rappé, A. K.; Casewit, C. J.; Colwell, K. S.; Goddard, W. A., III; Skiff, W. M. *J. Am. Chem. Soc.* **1992**, *114*, 10024.
(44) Vreven, T.; Morokuma, K. J. *J. Comput. Chem.* **2000**, *21*, 1419.
(45) Frisch, M. J.; Trucks, G. W.; Schlegel, H. B.; Scuseria, G. E.; Robb, M. A.; Cheeseman, J. R.; Montgomery, Jr., J. A.; Vreven, T.; Kudin, K. N.; Burant, J. C.; Millam, J. M.; Iyengar, S. S.; Tomasi, J.; Barone, V.; Mennucci, B.; Cossi, M.; Scalmani, G.; Rega, N.; Petersson, G. A.; Nakatsuji, H.; Hada, M.; Ehara, M.; Toyota, K.; Fukuda, R.; Hasegawa, J.; Ishida, M.; Nakajima, T.; Honda, Y.; Kitao, O.; Nakai, H.; Klene, M.; Li, X.; Knox, J. E.; Hratchian, H. P.; Cross, J. B.; Bakken, V.; Adamo, C.; Jaramillo, J.; Gomperts, R.; Stratmann, R. E.; Yazyev, O.; Austin, A. J.; Cammi, R.; Pomelli, C.; Ochterski, J. W.; Ayala, P. Y.; Morokuma, K.; Voth, G. A.; Salvador, P.; Dannenberg, J. J.; Zakrzewski, V. G.; Dapprich, S.; Daniels, A. D.; Strain, M. C.; Farkas, O.; Malick, D. K.; Rabuck, A. D.; Raghavachari, K.; Foresman, J. B.; Ortiz, J. V.; Cui, Q.; Baboul, A. G.; Clifford, S.; Cioslowski, J.; Stefanov, B. B.; Liu, G.; Liashenko, A.; Piskorz, P.; Komaromi, I.; Martin, R. L.; Fox, D. J.; Keith, T.; Al-Laham, M. A.; Peng, C. Y.; Nanayakkara, A.; Challacombe, M.; Gill, P. M. W.; Johnson, B.; Chen, W.; Wong, M. W.; González, C.; Pople, J. A. *Gaussian 03*, Revision C.02; Gaussian, Inc.: Wallingford, CT, 2004.
(46) Kooijman, H.; Spek, A. L.; van Bommel, K. J. C.; Verboom, W.; Reinhoudt, D. N. *Acta Crystallogr.* **1998**, *C54*, 1695.
(47) Blount, J. F.; Camp, D.; Hart, R. D.; Healy, P. C.; Skelton, B. W.; White, A. H. *Aust. J. Chem.* **1994**, *47*, 1631.
(48) Jones, P. G. *J. Chem. Soc., Chem. Commun.* **1980**, 1031.
(49) Zheng, L.; Yang, H.; Yang, W.; Zhang, Q. *Xiamen Dax. Xuebao, Zir. Kex.* **1990**, *29*, 421; (Chin) (J. Xiamen Univ. (Nat. Sci.)).
(50) Davidson, J. L.; Lindsell, W. E.; McCullough, K. J.; McInstosh, C. H. *Organometallics* **1995**, *14*, 3497.
(51) Staples, R. J.; King, C.; Khan, M. N. I.; Winpenny, R. E. P.; Fackler, J. P., Jr. *Acta Crystallogr.* **1993**, *C49*, 472.
(52) Bayler, A.; Schier, A.; Bowmaker, G. A.; Schmidbaur, H. *J. Am. Chem. Soc.* **1996**, *118*, 7006.
(53) *NBO*, Version 3.1; Glendening, E. D., Reed, A. E., Carpenter, J. E.; Weinhold, F., Eds.; Theoretical Chemistry Institute, University of Wisconsin : Madison, WI, 1987.
(54) Boys, S. F.; Bernardi, F. *Mol. Phys.* **1970**, *19*, 553.

Table 6. Selected Theoretical Structural Parameters, Dissociation Energies, and NBO s-Character on Sb or P for Free Ligands and Some Homoleptic Stibine- and Phosphine-Gold(I) Complexes $[Au(ER_3)_n]^+$ (E = P or Sb; R = Ph or Mes; n = 2, 3, or 4)

	Au−E	E−C	C−E−C	E_{dis}[a]	% of E s-charact.[b]
$SbPh_3$		2.18	97.2		10.75
$SbMes_3$		2.21	105.1		11.38
PPh_3		1.87	102.0−102.4		20.49
$[Au(SbPh_3)_2]^+$	2.63	2.10	104.2	53.1	28.38
$[Au(SbPh_3)_3]^+$	2.66−2.73	2.09−2.11	102.0−105.5	31.8	14.80
$[Au(SbPh_3)_4]^+$	2.71	2.10	103.6−103.8	14.2	14.60
$[Au(SbMes_3)_2]^+$	2.62	2.14	110.4	48.3	27.88
$[Au(PPh_3)_2]^+$	2.36	1.82	106.0	59.8	20.16
$[Au(PPh_3)_3]^+$	2.42−2.49	1.82−1.84	102.5−108.0	28.1	20.22
$[Au(PPh_3)_4]^+$	2.61−2.69	1.83−1.84	100.7−105.6	5.3	19.60

[a] Energy in kcal·mol^{-1}. [b] Mean P or Sb s-character in the Sb−C natural bond orbitals.

tetrahedral environment around gold(I) has been described. As we have mentioned before, when model systems with 2, 3, or 4 $SbPh_3$ ligands around gold are optimized, a local minimum is obtained in all cases, with Au−Sb distances within the range of a normal coordination bond. However, although a similar trend is observed for two- and three-coordinated triphenylphosphinegold(I) theoretical models (i.e., Au−P bonds in the range of coordination bonds, and similar Au−P dissociation energies to those of Au−Sb in the same coordination environments) (see Table 6), when the $[Au(PPh_3)_4]^+$ theoretical model is optimized a local minimum is reached at which the Au−P distances are at the bonding limit and the Au−P dissociation energy (5.34 kcal·mol^{-1}) appears very weak for a coordination bond. These results are also in accordance with the experimental observations. Thus, while the only known homoleptic triphenylstibinegold(I) cation is $[Au(SbPh_3)_4]^+$, a clear preference for two- or three-coordination is observed for Au(I) triphenylphosphine compounds.[13] In an early report, Jones characterized three modifications in the complex with stoichiometry $[Au(PPh_3)_4](BPh_4)$. The first of these being an $[Au(PPh_3)_3]^+$ moiety interacting over a large distance with the fourth PPh_3 ligand and, further, two disordered modifications with the possibility of tetrahedral coordination proposed at low temperature. Later, a new structure for the cation $[Au(PPh_3)_4]^+$ was described, but disorder in the structure was also found. The only remaining question at this point is the experimental preference for four-coordination $SbPh_3$ with Au(I) instead of two- or three-coordination, which, in principle, have higher dissociation energies. We have carried out several calculations of transition state optimizations to describe a possible kinetic preference for $[Au(SbPh_3)_4]^+$. In this sense, we were looking for a less energetic transition state for the fourth stibine coordination in contrast to the possibly more energetic transition states for second or third stibine coordination, but, unfortunately, we have not found any clear information for the moment.

Finally, both the analysis of the optimized structural parameters and the natural bond orbital analysis carried out for model systems $[Au(ER_3)_n]^+$ (E = P or Sb; R = Ph (n = 2, 3, or 4) or Mes (n = 2)) reveal very interesting information for the description of the effect of coordination on stibine ligand geometry previously proposed by Levason and co-workers, starting from a structural analysis. As was mentioned in the Introduction section of this work, one of the most striking features of stibine ligands is that on coordination to transition metal centers the C−Sb−C bond angles increase, whereas the Sb−C bond distances decrease. In Table 5 we summarize some of the structural data reported which shows this tendency for stibine-gold(I) complexes. In the case of stibine ligands Levason and co-workers have rationalized these effects.[8,55] If a hybridization model is considered, the increasing C−Sb−C angles on coordination correspond to increased s character in the Sb−C bond and increased p character in the "lone pair". In addition, when a Walsh diagram approach is chosen, σ-donation of the Sb "lone pair" upon coordination gives rise to a decreased population of the lone-pair orbital and, therefore, increased C−Sb−C angles (less pyramidalization) and decreased Sb−C distances. As can be observed in Table 6, the calculated C−Sb−C angles of $SbPh_3$ and $SbMes_3$ become larger when the ligands are coordinated to a Au(I) center in numbers of 2, 3, or 4 for $SbPh_3$ or 2 for $SbMes_3$, whereas the Sb−C distances get shorter in all cases, in agreement with the experimental data reported in this and previous works. A closer look at the Sb−C natural bonding orbital compositions for the free and coordinated ligands supports these trends (see Table 6). Thus, the Sb−C natural bond orbital analysis for free $SbPh_3$ and $SbMes_3$ displays a low s character on Sb (10.7% for $SbPh_3$ and 11.4% for $SbMes_3$) in agreement with predominant antimony p^3 hybridization. Upon coordination of the stibine ligands to gold(I) a clear increase in the s character on Sb (between 25 and 30% for two-coordinated stibines and around 15% for three- and four-coordinated $SbPh_3$) is observed, in agreement with a change in the antimony hybridization toward sp^3, which theoretically confirms the previously reported proposal.

In addition, systematic structural studies of the geometrical deformations of bonded PPh_3 fragments concluded that for phosphine complexes of late- and post-transition series metals, PPh_3 becomes less pyramidal (larger C−P−C angles and shorter P−C bond lengths).[56] If one focuses on gold(I)-PPh_3 complexes the latter trends are observed, leading to an analogous phenomena both for phosphine and stibine-gold(I) complexes. Nevertheless, when we analyze the natural bond orbitals for free and coordinated PPh_3 ligands, we observe a clear difference with stibines. In this case, both the free and the coordinated ligand display a high s character on P for the P−C bonds (around 20%). Therefore, it seems plausible that the slight geometrical changes of PPh_3 when it coordinates to gold(I) have a different origin, and we propose that the sp^3 character already present in the free phosphine ligands is retained upon coordination.

(55) Holmes, N. J.; Levason, W.; Webster, M. *J. Chem. Soc., Dalton Trans.* **1998**, 3457.
(56) Dunne, B. J.; Morris, R. B.; Orpen, A. G. *J. Chem. Soc., Dalton Trans.* **1991**, 653.

Conclusion

The use of stibine ligands with different aryl substituents (phenyl or mesityl) resulted in the isolation of the neutral 1:1 adducts [AuCl($SbMes_nPh_{3-n}$)] (n = 3 (**4**), 2 (**5**), 1 (**6**)), with a linear Sb−Au−Cl fragment, as well as the ionic 1:2 adducts [Au($SbMes_nPh_{3-n}$)$_2$]ClO_4 (n = 3 (**7**), 2 (**10**)) and [Au($SbMes_3$)$_2$]X (X = CF_3SO_3 (**8**), SbF_6 (**9**)), containing linear Sb−Au−Sb systems, and the 1:3 adduct [Au($SbMesPh_2$)$_3$]ClO_4 (**11**), with a *quasi* trigonal planar $AuSb_3$ core. The molecular structures of **4**, **7**, **8**·2$CDCl_3$, **9**, and **11** were established by single-crystal X-ray diffraction. Moreover, from the theoretical calculations we can establish some interesting conclusions:

(1) Homoleptic Au(I) theoretical models with $SbPh_3$ ligands are stable in linear, trigonal planar, and tetrahedral coordination environments. In contrast, the only stable Au(I) complex with $SbMes_3$ ligands is the dicoordinated (linear) one. For these aryl stibines gold coordination is governed by steric effects.

(2) Homoleptic Au(I) models with two, three, or four $SbPh_3$ ligands are within the same stability range and display similar Au−Sb bond distances. When the ligand is PPh_3 both the two- and three-coordinated models are stable and display normal Au−P distances, whereas the tetra-coordinated complex is rather less stable, showing larger Au−P distances. This theoretical trend is in agreement with the experimental preference for four $SbPh_3$ ligands bonded to gold(I), but for two or three PPh_3 ligands bonded to the same metal center.

(3) The theoretical calculations reproduce the experimental tendency already described for stibine ligands such that, upon coordination, the C−Sb−C angles increase and the Sb−C distances decrease. This trend is also confirmed for PPh_3 ligands bonded to Au(I).

(4) NBO analysis of the bonded stibines reflects the expected increase in s character of Sb with respect to the free ligands and, therefore, a change in the bonded antimony hybridization toward sp^3, also explaining the above-mentioned C−Sb−C and Sb−C distortions. Nevertheless, although the structural parameters of the PPh_3 ligand are also slightly changed upon coordination, the s character in the P atoms remains almost equal to that of the free ligand.

Experimental Section

Materials and Procedures. Most of the reactions and manipulations, except those otherwise mentioned, were carried out under an inert atmosphere (dry 99.99% argon) using Schlenk techniques. Solvents were dried using standard procedures and were freshly distilled prior to use. Starting materials such as $SbCl_3$, $SbPh_3$, MesMgBr (1 M solution in tetrahydrofuran) and $AgSbF_6$ were commercially available. $SbCl_3$ was freshly sublimed prior to use. The other starting materials were prepared according to the literature methods: $SbMes_3$ (**1**),[57] $SbPh_2Cl$,[58] $SbPhCl_2$,[59] [AuCl(tht)],[60] and [Au(tht)$_2$]X (X = ClO_4, CF_3SO_3).[61]

Instrumentation. Infrared spectra were recorded in the 4000−225 cm^{-1} range on a Nicolet Nexus FT-IR spectrophotometer with a CsI beam splitter, using Nujol mulls between polyethylene sheets. C, H analyses were carried out with a Perkin-Elmer 240C microanalyzer. NMR spectra were recorded in dried $CDCl_3$, at room temperature, on Bruker AVANCE 400 and Bruker ARX 300 spectrometers. The chemical shifts are reported in parts per million (ppm) relative to the residual peak of solvent [ref $CHCl_3$: δ(^{1}H) 7.26, δ(^{13}C) 77.0 ppm] for ^{1}H and ^{13}C NMR spectra, and relative to CCl_3F for ^{19}F NMR spectra. Mass spectra were recorded on HP5989B API-Electrospray, microOTOF-Q-Bruker (ES), and Microflex Bruker (MALDI) spectrometers.

Synthesis of $SbMes_2Ph$ (2). A MesMgBr solution (7.4 mL, 1 M solution in thf, 7.4 mmol) was added dropwise to a stirred suspension of $SbPhCl_2$ (1 g, 3.7 mmol) in thf (40 mL), cooled to −20 °C. The reaction mixture was stirred for 1 h at low temperature and then left to warm up to room temperature with stirring overnight. After removal of the solvent under vacuum, the remaining yellow oil was extracted with hexane. The hexane solution was filtered, and the solvent evaporated resulting in the title compound as a white solid. Yield: 1.23 g (76%). Mp 78−79 °C. Elemental analysis calcd (%) for $C_{24}H_{27}Sb$: C 65.93, H 6.22; found: C 65.45, H 6.12; ^{1}H NMR: δ = 2.25 (s, 12H; CH_3-*ortho*), 2.28 (s, 6H; CH_3-*para*), 6.85 (s, 4H; C_6H_2), 7.25 (m, 3H; C_6H_5-*meta*+*para*), 7.59 (m, 2H; C_6H_5-*ortho*); ^{13}C NMR: δ = 20.91 (CH_3-*para*), 25.77 (CH_3-*ortho*), 127.87 (C_6H_5-*para*), 128.36 (C_6H_5-*meta*), 128.80 (C_6H_2-*meta*), 135.97 (C_6H_2-*ipso*), 136.84 (C_6H_5-*ortho*), 137.76 (C_6H_5-*ipso*), 138.08 (C_6H_2-*para*), 144.51 (C_6H_2-*ortho*); ES+/MS (CH_3OH/H_2O): m/z (%) 438 (100) $[M]^+$.

Synthesis of $SbMesPh_2$ (3). A MesMgBr solution (2 mL, 1 M solution in thf, 2 mmol) was added dropwise to a stirred suspension of $SbPh_2Cl$ (0.625 g, 2 mmol) in thf (40 mL), cooled to −20 °C. The reaction mixture was stirred for 1 h at low temperature and then left to warm up to room temperature with stirring overnight. The solvent was removed under vacuum, and the remaining yellow-white oily mixture was extracted with hexane. The hexane solution was filtered, and evaporation of the solvent resulted in the title compound as a white crystalline solid. Yield: 0.53 g (67%). Mp 82−84 °C. Elemental analysis calcd (%) for $C_{21}H_{21}Sb$: C 63.83, H 5.36; found: C 64.00, H 5.40; ^{1}H NMR: δ = 2.28 (s, 6H; CH_3-*ortho*), 2.33 (s, 3H; CH_3-*para*), 6.94 (s, 2H; C_6H_2), 7.34 (m, 6H; C_6H_5-*meta*+*para*), 7.56 (m, 4H; C_6H_5-*ortho*); ^{13}C NMR: δ = 21.01 (CH_3-*para*), 26.45 (CH_3-*ortho*), 128.10 (C_6H_5-*para*), 128.75 (C_6H_5-*meta*), 128.93 (C_6H_2-*meta*), 134.81 (C_6H_2-*ipso*), 135.57 (C_6H_5-*ortho*), 137.69 (C_6H_5-*ipso*), 139.01 (C_6H_2-*para*), 145.76 (C_6H_2-*ortho*); ES+/MS (CH_3OH/H_2O): m/z (%) 412 (95) $[M + OH]^+$, 396 (100) $[M]^+$, 276 (90) $[SbPh_2]^+$.

Synthesis of [AuCl($SbMes_3$)] (4). Solid $SbMes_3$ (0.224 g; 0.46 mmol) was added to a solution of [AuCl(tht)] (0.15 g; 0.46 mmol) in dichloromethane (25 mL) at room temperature. The mixture was stirred for 5 min. Evaporation of the solvent under reduced pressure resulted in an oily, white residue which solidifies on addition of hexane. Colorless crystals were obtained from a dichloromethane/hexane mixture. Yield: 0.275 g (82%). Elemental analysis calcd (%) for $C_{27}H_{33}AuClSb$: C 45.56, H 4.67; found: C 45.22, H 4.32; ^{1}H NMR: δ = 2.29 (s, 9H; CH_3-*para*), 2.42 (s, 18H; CH_3-*ortho*), 6.91 (s, 6H; C_6H_2); ^{13}C NMR: δ = 20.90 (CH_3-*para*), 25.96 (CH_3-*ortho*), 130.32 (C_6H_2-*ipso*),

(57) *Synthetic Methods of Organometallic and Inorganic Chemistry*; Hermann, W. A., Karsch, H. H., Eds.; G. Thieme Verlag: Stuttgart, 1996; Vol. *3* − Phosphorus, Arsenic, Antimony and Bismuth, p 204.
(58) Becker, G.; Mundt, O.; Sachs, M.; Breunig, H. J.; Lork, E.; Probst, J.; Silvestru, A. *Z. Anorg. Allg. Chem.* **2001**, *627*, 699.
(59) Nunn, M.; Sowerby, D. B.; Wesolek, D. M. *J. Organomet. Chem.* **1983**, *251*, C45.
(60) Usón, R.; Laguna, A.; Laguna, M. *Inorg. Synth.* **1989**, *26*, 85.
(61) Usón, R.; Laguna, A.; Laguna, M.; Jiménez, J.; Gómez, M. P.; Sainz, A.; Jones, P. G. *J. Chem. Soc., Dalton Trans.* **1990**, 3457.

130.43 (C_6H_2-*meta*), 140.73 (C_6H_2-*para*), 143.62 (C_6H_2-*ortho*); FT-IR (nujol mulls): 326 cm^{-1} [ν(Au−Cl)]; ES+/MS (CH_3OH/H_2O): *m*/*z* (%) 1155 (100) $[Au(SbMes_3)_2]^+$, 495 (34) $[Mes_3SbO]^+$.

Synthesis of [AuCl(SbMes$_2$Ph)] (5). Same procedure as for **4**, from solid $SbMes_2Ph$ (0.201 g; 0.46 mmol) added to a solution of [AuCl(tht)] (0.15 g; 0.46 mmol) in dichloromethane (25 mL) at room temperature. The oily, white reaction product obtained after evaporation of the solvent under reduced pressure, solidifies on addition of hexane. Yield: 0.234 g (76%). Elemental analysis calcd (%) for $C_{24}H_{27}AuClSb\cdot 2CH_2Cl_2$: C 37.20, H 3.72; found: C 37.19, H 3.65; ^{1}H NMR: δ = 2.29 (s, 6H; CH_3-*para*), 2.35 (s, 12H; CH_3-*ortho*), 6.92 (s, 4H; C_6H_2), 7.41 (m, 3H; C_6H_5-*meta*+*para*), 7.71 (m, 2H; C_6H_5-*ortho*); ^{13}C NMR: δ = 20.98 (CH_3-*para*), 25.88 (CH_3-*ortho*), 128.30 (C_6H_2-*ipso*), 129.75 (C_6H_5-*meta*), 130.28 (C_6H_2-*meta*), 130.78 (C_6H_5-*para*), 131.88 (C_6H_5-*ipso*), 136.01 (C_6H_5-*ortho*), 141.05 (C_6H_2-*para*), 143.37 (C_6H_2-*ortho*); FT-IR (nujol mulls): 321 cm^{-1} [ν(Au−Cl)]; ES+/MS (CH_3OH/H_2O): *m*/*z* (%) 1103 (10) $[Au(SbMes_2Ph)_2 + CH_3OH]^+$, 1071 (100%) $[Au(SbMes_2Ph)_2]^+$; 453 (3) $[PhMes_2SbO]^+$.

Synthesis of [AuCl(SbMesPh$_2$)] (6). Same procedure as for **4**, from solid $SbMesPh_2$ (0.1817 g; 0.46 mmol) added to a solution of [AuCl(tht)] (0.15 g; 0.46 mmol) in dichloromethane (25 mL) at room temperature. The oily, white reaction product obtained after evaporation of the solvent under reduced pressure, solidifies on addition of diethyl ether. Colorless crystals were obtained from a chloroform/hexane mixture. Yield: 0.345 g (72%). Elemental analysis calcd (%) for $C_{21}H_{21}AuClSb\cdot CHCl_3$: C 35.37, H 2.97; found: C 35.05, H 3.09; ^{1}H NMR: δ = 2.27 (s, 6H; CH_3-*ortho*), 2.32 (s, 3H; CH_3-*para*), 6.94 (s, 2H; C_6H_2), 7.44 (m, 6H; C_6H_5-*meta*+*para*), 7.60 (d, 4H, *J*(H,H) = 7.4 Hz; C_6H_5-*ortho*); ^{13}C NMR: δ = 21.03 (CH_3-*para*), 26.15 (CH_3-*ortho*), 125.32 (C_6H_2-*ipso*), 129.90 (C_6H_5-*meta*), 130.32 (C_6H_2-*meta*), 130.89 (C_6H_5-*ipso*), 130.92 (C_6H_5-*para*), 135.34 (C_6H_5-*ortho*), 141.69 (C_6H_2-*para*), 144.58 (C_6H_2-*ortho*); FT-IR (nujol mulls): 321 cm^{-1} [ν(Au−Cl)]; ES+/MS (CH_3OH/H_2O): *m*/*z* (%) 986 (100) $[Au(SbMesPh_2)_2]^+$, 453 (57) $[PhMes_2SbO]^+$, 411 (9%) $[SbMesPh_2 + CH_3]^+$.

Synthesis of [Au(SbMes$_3$)$_2$]ClO$_4$ (7). Solid $SbMes_3$ (0.2025 g; 0.42 mmol) was added to a clear solution of $[Au(tht)_2]ClO_4$ (0.1 g; 0.21 mmol) in dichloromethane (25 mL) at room temperature. The reaction mixture was stirred for 5 min, when the solution turned pale yellow and slowly started to decompose. Fast evaporation of the solvent and addition of hexane (10 mL) resulted in isolation of the title compound as a white solid. Colorless crystals were obtained from a dichloromethane/hexane mixture. Yield: 0.235 g (88%). Elemental analysis calcd (%) for $C_{54}H_{66}AuClO_4Sb_2$: C 51.68, H 5.30; found: C 51.79, H 5.02;^{1}H NMR: δ = 2.30 (s, 54H; CH_3-*ortho*+*para*), 6.95 (s, 12H; C_6H_2); ^{13}C NMR: δ = 20.92 (CH_3-*para*), 25.75 (CH_3-*ortho*), 130.50 (C_6H_2-*ipso*), 130.83 (C_6H_2-*meta*), 141.52 (C_6H_2-*para*), 143.13 (C_6H_2-*ortho*); FT-IR (nujol mulls): 1095, 623 cm^{-1} [$\nu(ClO_4)$]; ES+/MS (CH_3OH/H_2O): *m*/*z* (%) 1155 (100) $[Au(SbMes_3)_2]^+$, 495 (52) $[Mes_3SbO]^+$; ES−/MS (CH_3OH/H_2O): *m*/*z* (%)99 (100%) $[ClO_4]^-$.

Synthesis of [Au(SbMes$_3$)$_2$]CF$_3$SO$_3$ (8). Same procedure as for **7**, from solid $SbMes_3$ (0.1832 g; 0.38 mmol) added to a solution of $[Au(tht)_2]CF_3SO_3$ (0.1 g; 0.19 mmol) in dichloromethane (25 mL) at room temperature. Fast evaporation of the solvent and addition of hexane (10 mL) resulted in isolation of the title compound as a white solid. Colorless crystals were obtained from a dichloromethane/hexane mixture. Yield: 0.237 g (95%). Elemental analysis calcd (%) for $C_{55}H_{66}AuF_3O_3SSb_2$: C 50.63, H 5.10; found: C 50.59, H 5.06; ^{1}H NMR: δ = 2.30 (br s, 54H; CH_3-*ortho*+*para*), 6.95 (s, 12H; C_6H_2); ^{13}C NMR: δ = 20.94 (CH_3-*para*), 25.77 (CH_3-*ortho*), 130.53 (C_6H_2-*ipso*), 130.86 (C_6H_2-*meta*), 141.58 (C_6H_2-*para*), 143.17 (C_6H_2-*ortho*); ^{19}F NMR: δ = −120.61; MALDI+/MS (HCCA): *m*/*z* (%) 1155 (100) $[Au(SbMes_3)_2]^+$.

Synthesis of [Au(SbMes$_3$)$_2$]SbF$_6$ (9). Solid $AgSbF_6$ (0.012 g, 0.035 mmol) was added to a clear solution of [AuCl($SbMes_3$)] (**4**) (0.05 g, 0.07 mmol) in dichloromethane (20 mL) in an Al foil wrapped flask for light protection. The AgCl is formed rapidly as a white precipitate which turns slowly into dark gray. After 5 min the reaction mixture was filtered off, and the solvent was removed under vacuum from the resulting colorless solution. The title compound was isolated as a white solid on addition of hexane (10 mL). Colorless crystals were obtained from a dichloromethane/hexane mixture. Yield: 0.022 g (46%). Elemental analysis calcd (%) for $C_{54}H_{66}AuF_6Sb_3$: C 46.62, H 4.78; found: C 46.52, H 4.69; ^{1}H NMR: δ = 2.31 (br s, 54H; CH_3-*ortho*+*para*), 6.96 (s, 12H; C_6H_2); ^{13}C NMR: δ = 20.93 (CH_3-*para*), 25.76 (CH_3-*ortho*), 130.56 (C_6H_2-*ipso*), 130.86 (C_6H_2-*meta*), 141.57 (C_6H_2-*para*), 143.18 (C_6H_2-*ortho*); ^{19}F NMR: δ = −120.44.

Synthesis of [Au(SbMes$_2$Ph)$_2$]ClO$_4$ (10). Same procedure as for **7**, from solid $SbMes_2Ph$ (0.1835 g; 0.42 mmol) added to a solution of $[Au(tht)_2]ClO_4$ (0.1 g; 0.21 mmol) in dichloromethane (20 mL) at room temperature. Fast evaporation of the solvent and addition of diethyl ether (10 mL) resulted in isolation of the title compound as a white solid. Yield: 0.168 g (68%). Elemental analysis calcd (%) for $C_{48}H_{54}AuClO_4Sb_2$: C 49.24, H 4.65; found: C 49.77, H 4.51; ^{1}H NMR: δ = 2.13 (s, 24H; CH_3-*ortho*), 2.30 (s, 12H; CH_3-*para*), 6.87 (s, 8H; C_6H_2), 7.17 (t, 4H *J*(H,H) = 7.5 Hz; C_6H_5-*meta*), 7.34 (m, 6H; C_6H_5-*ortho*+*para*); ^{13}C NMR: δ = 20.98 (CH_3-*para*), 25.88 (CH_3-*ortho*), 129.57 (C_6H_5-*meta*), 130.23 (C_6H_2-*ipso*+*meta*), 131.23 (C_6H_5-*ipso*), 133.61 (C_6H_5-*para*), 135.59 (C_6H_5-*ortho*), 140.74 (C_6H_2-*para*), 143.55 (C_6H_2-*ortho*); ES+/MS (CH_3OH/H_2O): *m*/*z* (%) 1071 (19%) $[Au(SbMes_2Ph)_2]^+$; 473 (6) $[AuSbPh_2]^+$, 453 (100) $[PhMes_2SbO]^+$; ES−/MS (CH_3OH/H_2O): *m*/*z* (%)99 (100%) $[ClO_4]^-$.

Synthesis of [Au(SbMesPh$_2$)$_3$]ClO$_4$ (11). Solid $SbMesPh_2$ (0.2488 g; 0.63 mmol) was added to a clear solution of $[Au(tht)_2]ClO_4$ (0.1 g; 0.21 mmol) in dichloromethane (20 mL) at room temperature. The reaction mixture was stirred for 5 min, when the solution turned pale yellow and slowly started to decompose. Fast evaporation of the solvent and addition of hexane (10 mL) resulted in isolation of the title compound as a white solid. Colorless crystals were obtained from a dichloromethane/hexane mixture. Yield: 0.265 g (85%). Elemental analysis calcd (%) for $C_{63}H_{63}AuClO_4Sb_3\cdot CH_2Cl_2$: C 49.06, H 4.18; found: C 49.22, H 4.10; ^{1}H NMR: δ = 2.03 (s, 18H; CH_3-*ortho*), 2.34 (s, 9H; CH_3-*para*), 6.91 (s, 6H; C_6H_2), 7.21 (m, 18H; C_6H_5-*meta*+*para*), 7.39 (m, 12H; C_6H_5-*ortho*); ^{13}C NMR: δ = 21.05 (CH_3-*para*), 26.00 (CH_3-*ortho*), 129.02 (C_6H_2-*ipso*), 129.78 (C_6H_5-*ipso*), 129.95 (C_6H_5-*meta*), 130.32, 130.54 (C_6H_2-*meta*, C_6H_5-*para*), 134.89 (C_6H_5-*ortho*), 141.46 (C_6H_2-*para*), 144.26 (C_6H_2-*ortho*); FT-IR (nujol mulls): 1093, 623 cm^{-1} [$\nu(ClO_4)$]; ES+/MS (CH_3OH/H_2O): *m*/*z* (%) 986 (45) $[Au(SbMesPh_2)_2]^+$, 513 (89%) $[SbMesPh_2 + Mes]^+$; 453 (1) $[PhMes_2SbO]^+$, 430 (100%) $[SbMesPh_2 + CH_3OH]^+$, 411 (9%) $[SbMesPh_2 + CH_3]^+$; ES−/MS (CH_3OH/H_2O): *m*/*z* (%)99 (100%) $[ClO_4]^-$.

Computational Details. All calculations were performed using the Gaussian 03 suite of programs.[45] Hybrid DFT-B3LYP/molecular mechanical (Universal Force Field, UFF)[44] (QM/MM) ONIOM calculations[43] were carried out for model systems of the type ER_3 and $[Au(ER_3)_n]^+$ (E = P or Sb; R = Ph or Mes; *n* = 2, 3, or 4). The quantum mechanical part was the cation core $[Au(EH_3)_n]^+$ (E = P or Sb, *n* = 2, 3, or 4) and was fully optimized at DFT-B3LYP level. The molecular mechanics parts are the Ph or Mes rings on the Sb or P atoms, and they were treated with the Universal Force Field. No symmetry constrains were included. After full optimization a single point DFT-B3LYP calculation was carried out for all model systems including the aromatic rings in the calculation. NBO[53] analysis was performed in all cases. The Au−E bond dissociation

Table 7. Details of Data Collection and Structure Refinement for Compounds **2**, **3**, and **4**

	2	**3**	**4**
chemical formula	$C_{21}H_{21}Sb$	$C_{24}H_{27}Sb$	$C_{27}H_{33}AuClSb$
crystal habit	colorless block	colorless block	colorless block
crystal size [mm]	0.38 × 0.32 × 0.28	0.51 × 0.23 × 0.16	0.60 × 0.60 × 0.60
crystal system	orthorhombic	monoclinic	orthorhombic
space group	$P2_12_12_1$	$C2/c$	$Pbca$
a [Å]	11.845(6)	21.369(3)	15.2821(9)
b [Å]	11.854(6)	13.7360(16)	17.2830(12)
c [Å]	12.943(6)	14.5729(17)	19.0543(8)
β [deg]	90	102.300(2)	90
V [Å^3]	1817.4(16)	4179.3(9)	5032.6(5)
Z	4	8	8
ρ_{calcd} [g cm^{-3}]	1.444	1.390	1.879
M_r	395.13	437.21	711.70
$F(000)$	792	1776	2736
T [K]	297(2)	297(2)	100(2)
$2\theta_{max}$ [deg]	50.0	50.0	60.1
$\mu(Mo_{K\alpha})$ (mm^{-1})	1.513	1.323	7.015
no. of reflections measured	9493	14857	54928
no. of unique reflections	3185	367	7166
R_{int}	0.087	0.057	0.057
R_1 ($I > 2\sigma(I)$)	0.054	0.064	0.026
wR_2	0.122	0.1243	0.059
no. of parameters	202	232	280
no. of restraints	0	0	96
GOF on F^2	1.07	1.20	1.11
largest diff. electron density [e Å^{-3}]	0.89/−1.52	0.84/−0.93	0.98/−1.28

Table 8. Details of Data Collection and Structure Refinement for Compounds **7**, **8**·2CDCl$_3$, **9**, and **11**

	7	**8**·2CDCl$_3$	**9**	**11**
chemical formula	$C_{54}H_{66}AuClO_4Sb_2$	$C_{57}H_{68}AuCl_6F_3O_3Sb_2$	$C_{54}H_{66}AuF_6Sb_3$	$C_{63}H_{63}AuClO_4Sb_3$
crystal habit	prismatic needle	colorless needle	colorless block	colorless prism
crystal size [mm]	0.20 × 0.05 × 0.05	0.30 × 0.10 × 0.05	0.23 × 0.25 × 0.30	0.25 × 0.22 × 0.10
crystal system	trigonal	monoclinic	trigonal	cubic
space group	$P3_12_1$	$P2_1/c$	$P3_12_1$	$Pa\bar{3}$
a [Å]	15.2038(3)	14.0282(3)	15.574(8)	22.1544(3)
b [Å]	15.2038(3)	17.8474(5)	15.574(8)	22.1544(3)
c [Å]	19.1083(4)	24.6533(6)	20.34(2)	22.1544(3)
β [deg]	90	94.621(2)	90	90
V [Å^3]	3825.22(13)	6152.3(3)	4273(5)	10873.8(3)
Z	3	4	3	8
ρ_{calcd} [g cm^{-3}]	1.634	1.666	1.622	1.810
M_r	1254.98	1543.34	1391.28	1481.80
$F(000)$	1860	3040	2028	5766
T [K]	173(2)	173(2)	297(2)	293(2)
$2\theta_{max}$ [deg]	54.9	55.0	50.0	54.9
$\mu(Mo_{K\alpha})$ (mm^{-1})	4.016	3.595	4.025	4.262
no. of reflections measured	47807	74483	30416	4519
no. of unique reflections	5846	13821	5038	4009
R_{int}	0.107	0.102	0.067	0.030
R_1 ($I > 2\sigma(I)$)	0.039	0.046	0.077	0.051
wR_2	0.065	0.077	0.152	0.141
no. of parameters	290	684	300	220
no. of restraints	96	132	81	72
GOF on F^2	1.03	1.02	1.32	1.16
largest diff. electron density [e Å^{-3}]	1.21/−0.79	0.87/−0.96	1.21/−2.09	4.81/−1.78

energies were estimated using counterpoise correction for the Basis Set Superposition Error (BSSE).[54] The 19-valence electron (VE) quasirelativistic (QR) pseudopotential (PP) of Andrae[62] was employed for gold together with two f-type polarization functions (exponents: 0.2, 1.19). The atoms Sb, P, and C were treated by Stuttgart pseudopotentials,[63] including only the valence electrons for each atom. For these atoms double-ζ basis sets of ref 63 were used, augmented by d-type polarization functions.[64] For the H atom, a double-ζ, plus a p-type polarization function was used.[65]

Crystallography. For single crystal X-ray diffraction the data were collected using Bruker SMART APEX (Babes-Bolyai University, Cluj-Napoca) (**2**, **3**, **9**) or Nonius Kappa CCD (Universidad de La Rioja, Logroño) (**4**, **7**, **8**·2CDCl$_3$, **11**) diffractometers, with graphite-monochromator Mo−Kα radiation (λ = 0.71073 Å), at 297 and 173 K (cooled under a nitrogen stream), respectively. The crystals were attached to a glass fiber with epoxy glue or Kel-F oil (for the low temperature measurements). The structures were refined with anisotropic displacement ellipsoids. Hydrogen atoms were included using a riding

(62) Andrae, D.; Häusserman, U.; Dolg, M.; Stoll, H.; Preuss, H. *Theor. Chim. Acta* **1990**, *77*, 123.
(63) Bergner, A.; Dolg, M.; Küchle, W.; Stoll, H.; Preuss, H. *Mol. Phys.* **1993**, *80*, 1431.
(64) Huzinaga, S. *Gaussian Basis Sets for Molecular Calculations*; Elsevier: Amsterdam, 1984; p 16.
(65) Huzinaga, S. *J. Chem. Phys.* **1965**, *42*, 1293.

model. The large residual electron density found in the crystal structure of **11** is probably due to the presence of disordered solvent that could not be solved. The absolute structure for **7** and **9** was determined refining the Flack (χ) parameter: 0.019(5) in **7** and 0.068(13) for **9**. For structure solving and refinement the software package SHELX-97 was used.[66] Further details of the data collection are given in Tables 7 and 8. The drawings were created with the DIAMOND program by Crystal Impact GbR.[67] Crystallographic data (excluding structure factors) for the structures reported in this paper have been deposited with the Cambridge Crystallographic Data Centre as supplementary publication nos. CCDC-764762−764768. Copies of the data can be obtained free of charge on application to CCDC, 12 Union Road, Cambridge CB2 1EZ, U.K. (fax: (0.44) 1223−336−033; e-mail: deposit@ccdc.cam.ac.uk).

(66) Sheldrick, G. M. *Acta Crystallogr*. **2008**, *A64*, 112.
(67) *DIAMOND − Visual Crystal Structure Information System*; Crystal Impact: Postfach 1251, 53002 Bonn, Germany, 2001.

Acknowledgment. Financial support from the Spanish MICINN (CTQ-2007-67273-C02-02), Ministry of Education and Research of Romania (Excellency Research Program, Research Project CEx-D11-16/2005; Project 19/2006) and National University Research Council (CNCSIS, Romania; Research Project Nos. A-709/2006, TD-397/2006 and ID-2052/2009) is greatly appreciated. V.R.B. thanks the Universidad de La Rioja for providing research facilities and financial support during short-term research stays. We also thank the National Center for X-ray Diffraction (Babes-Bolyai University, Cluj-Napoca, Romania) for the support in the solid state structure determinations.

Supporting Information Available: X-ray crystalloraphic data of compounds **2**−**4**, **7**, **8**·2$CDCl_3$, **9**, and **11** in cif format. Figures S1−S11 represent the 3D arrangement of **4**, **7**−**9**. Figures S12−S18 summarize theoretical results. This material is available free of charge via the Internet at http://pubs.acs.org.